**DEUTSCHES ELEKTRONEN-SYNCHROTRON**
**Ein Forschungszentrum der Helmholtz-Gemeinschaft**

DESY 19-141
OUTP-19-10P
TTK-19-46
arXiv:1911.03176
November 2019

# Invisible and Displaced Dark Matter Signatures at Belle II

M. Duerr

*Rudolf Peierls Centre for Theoretical Physics,*
*University of Oxford, Clarendon Laboratory, UK*

T. Ferber, K. Schmidt-Hoberg

*Deutsches Elektronen-Synchrotron DESY, Hamburg*

C. Hearty

*Department of Physics and Astronomy, and Institute of Particle Physics,*
*University of British Columbia, Vancouver, Canada*

F. Kahlhoefer, P. Tunney

*Institut für Theoretische Teilchenphysik und Kosmologie,*
*RWTH Universität Aachen*

ISSN 0418-9833

**NOTKESTRASSE 85 - 22607 HAMBURG**

Prepared for submission to JHEP

# Invisible and displaced dark matter signatures at Belle II

**Michael Duerr, Torben Ferber, Christopher Hearty, Felix Kahlhoefer, Kai Schmidt-Hoberg, and Patrick Tunney**

1

2
3

4

Abstract:

Keywords:

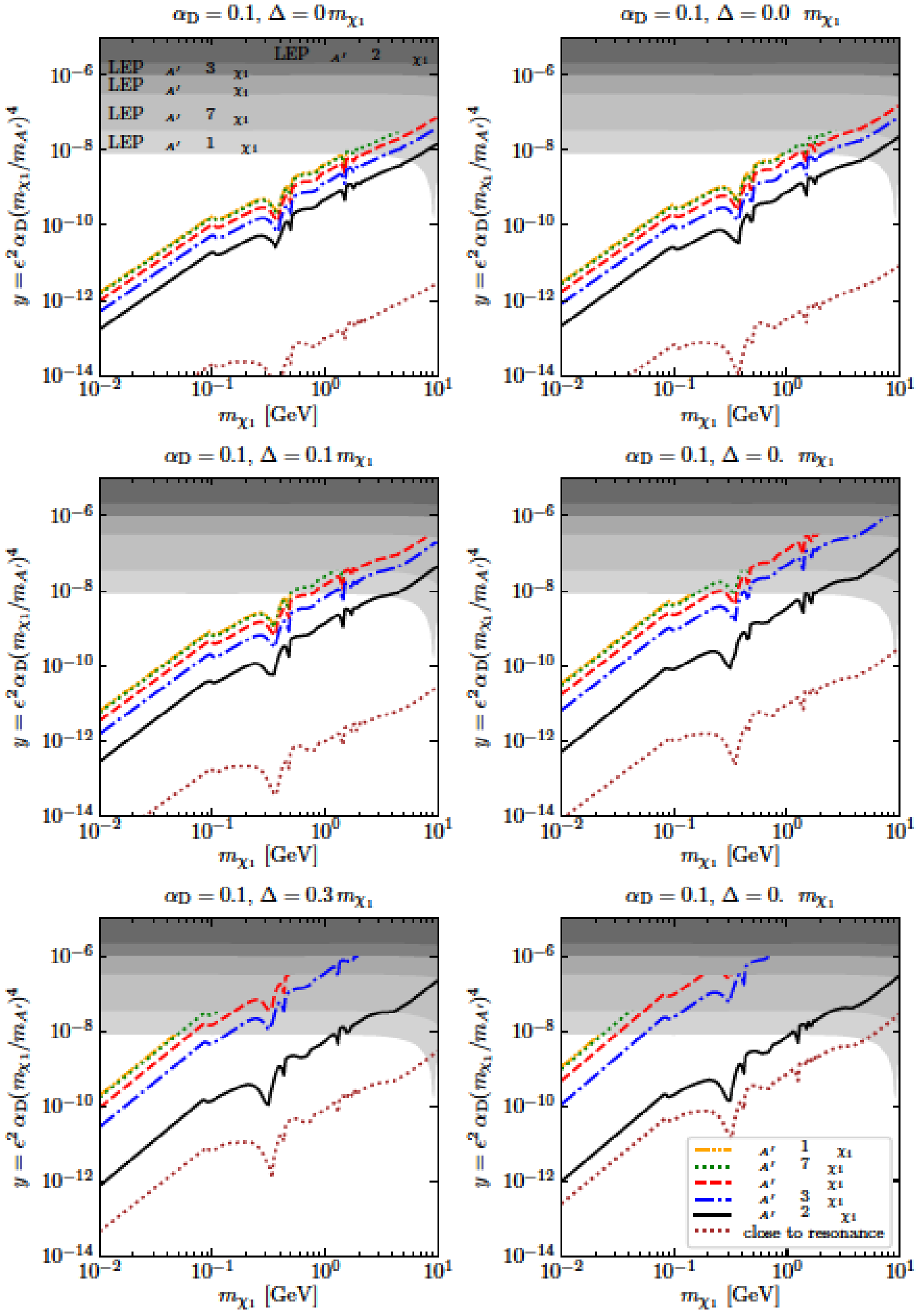


**Figure 1**: Thermal targets ($\Omega_{\rm DM}h^2 = 0.12$ [23]) for the inelastic DM model. We show various DM mass differences $\Delta/m_{\chi_1} = [0, 0.05, 0.1, 0.2, 0.3, 0.4]$ (different panels) and various mediator mass ratios $m_{A'}/m_{\chi_1} = [2.5, 3, 4, 7, 10]$ (different lines in each panel). For the line labelled 'close to resonance' the mediator mass is set to $m_{A'} = 2.01\, m_{\chi_1} + \Delta$. The model-independent LEP bound [41] on the kinetic mixing parameter $\epsilon$ constrains values of $\epsilon \approx 3 \times 10^{-2}$ away from the $Z$ resonance and hence results in a different limit on $y$ for differing ratios of $m_{A'}/m_{\chi_1}$.

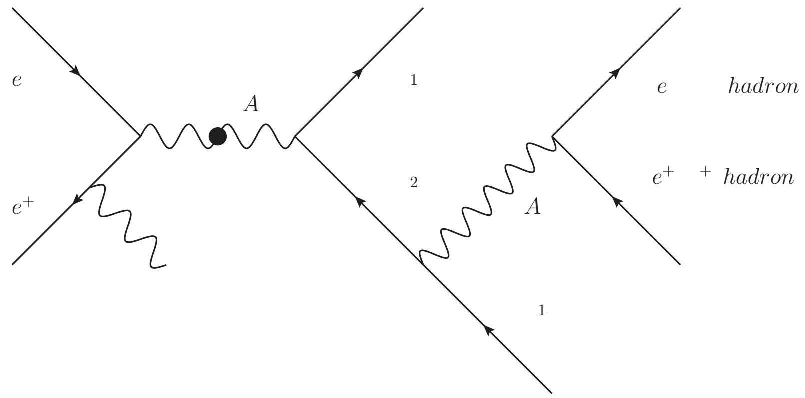

e
e+
A
1
2
A
1
e
hadron
e+
+ hadron


–

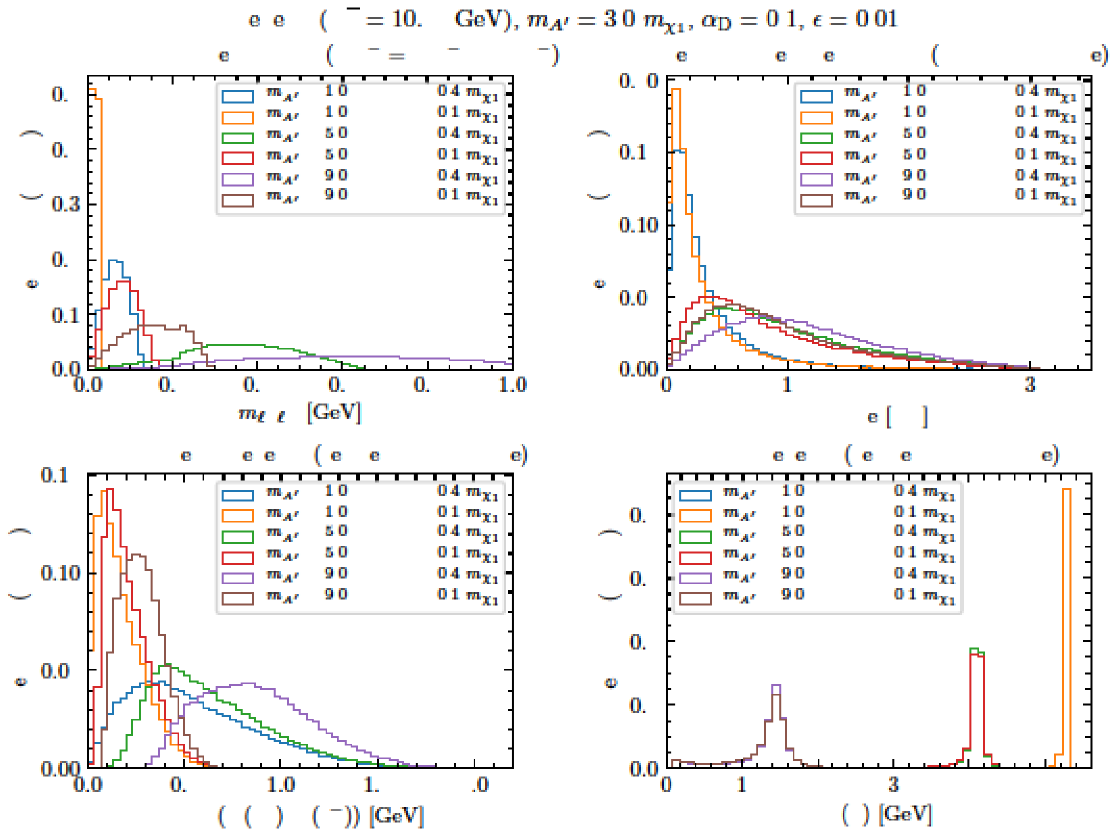

**Figure 3**: Histograms of various observables for our signal (top left: invariant mass of the lepton pair, top right: opening angle of the lepton pair, bottom left: maximum lepton energy, bottom right: photon energy). Note that the opening angle is given in the Belle II lab frame, whereas the maximum lepton energy and the photon energy are given in the centre-of-mass frame in this figure and in the text. In the lower right panel, the curves for $\Delta = 0.4\, m_{\chi_1}$ and $\Delta = 0.1\, m_{\chi_1}$ for $m_{A'} = 1\,\text{GeV}$ completely overlap.

$E_{\text{CMS}}(\gamma) > 0.1\,\text{GeV}$ and a maximal rapidity of the photon $\eta_{\text{max}} = 2.028698$ in the centre-of-mass frame.

We point out a number of relevant features:

- The invariant mass of the di-lepton pair must satisfy the requirement $m_{\ell^+\ell^-} \leq \Delta$ and typically peaks at around half of this value.
- The opening angle of the di-lepton pair in the laboratory frame depends sensitively on the boost (and hence the mass) of $\chi_2$, i.e. lighter $\chi_2$ will have higher boost and hence lead to smaller opening angles of the di-lepton pair.
- The maximum lepton energy is a combination of the two previous effects, i.e. it increases both with the mass splitting and with the boost of the $\chi_2$.

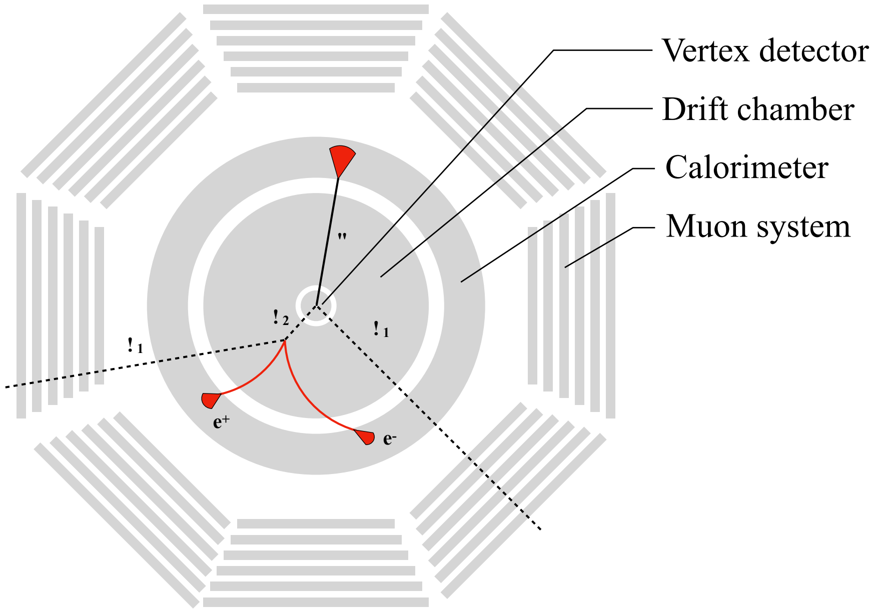
Vertex detector
Drift chamber
Calorimeter
Muon system
e+
e-

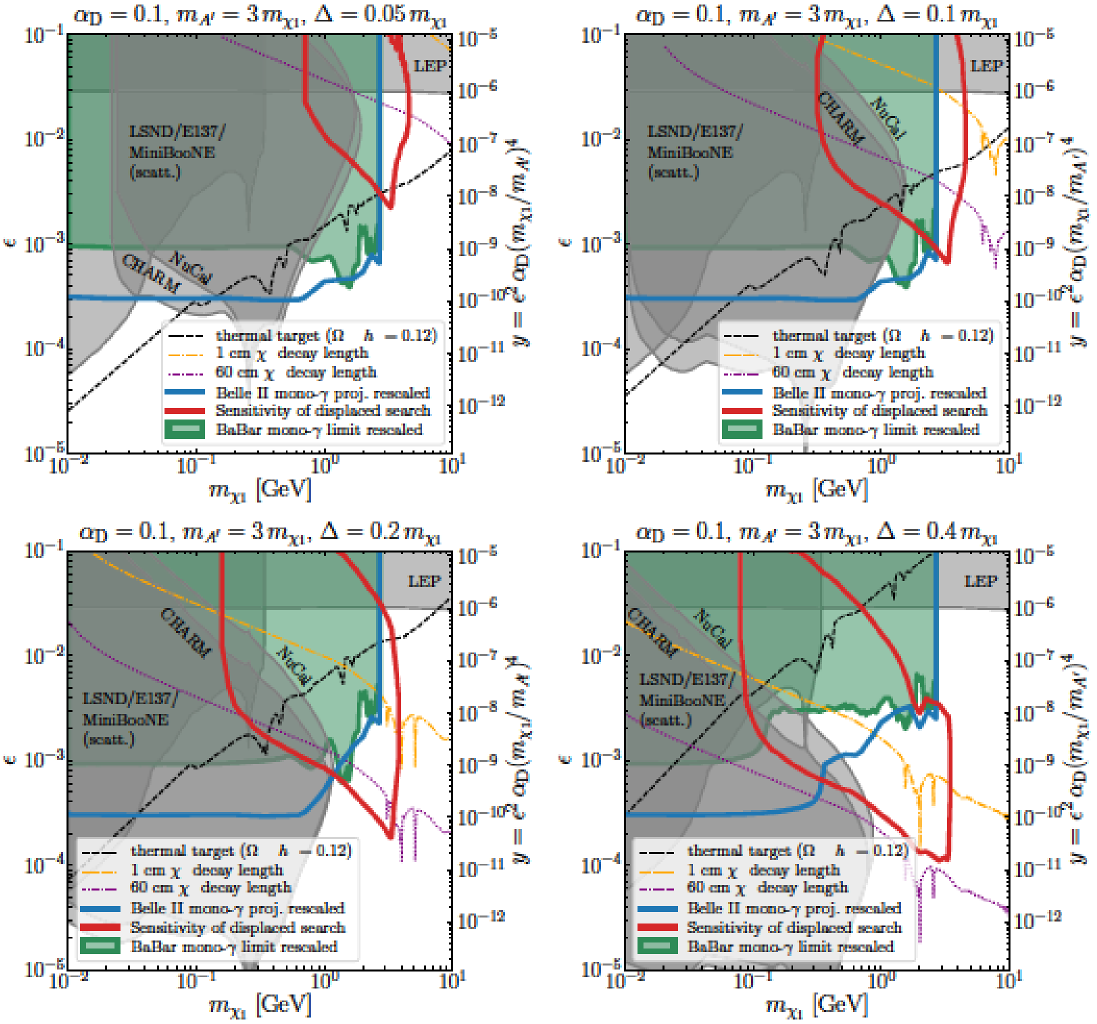


**Figure 5**: Sensitivity of Belle II to the parameter space of inelastic DM for an integrated luminosity of 20 fb$^{-1}$ for $m_{A'} = 3\,m_{\chi_1}$.

We make the following observations: For small mass splitting $\Delta$, corresponding to large decay length of $\chi_2$ the bound from BaBar and the projected sensitivity of the mono-photon search at Belle II are very similar to the ones obtained for invisibly decaying dark photons, because the $\chi_2$ simply escapes from the detector before decaying. As soon as the decay length of the $\chi_2$ becomes comparable to the size of the detector, the sensitivity of these searches is significantly suppressed. Note that the bound does however not disappear entirely even for very short-lived $\chi_2$. The reason is that there always is a non-zero probability that the particles produced in the $\chi_2$ decay have very little transverse momentum (i.e. they travel in the direction of the beam pipe) and will not be reconstructed, so that the event resembles a single-photon event. The BaBar bound that we obtain is therefore considerably stronger than the one from Ref. [27], where no requirement on the angle $\theta_{\rm lab}$ of the vertex is imposed.

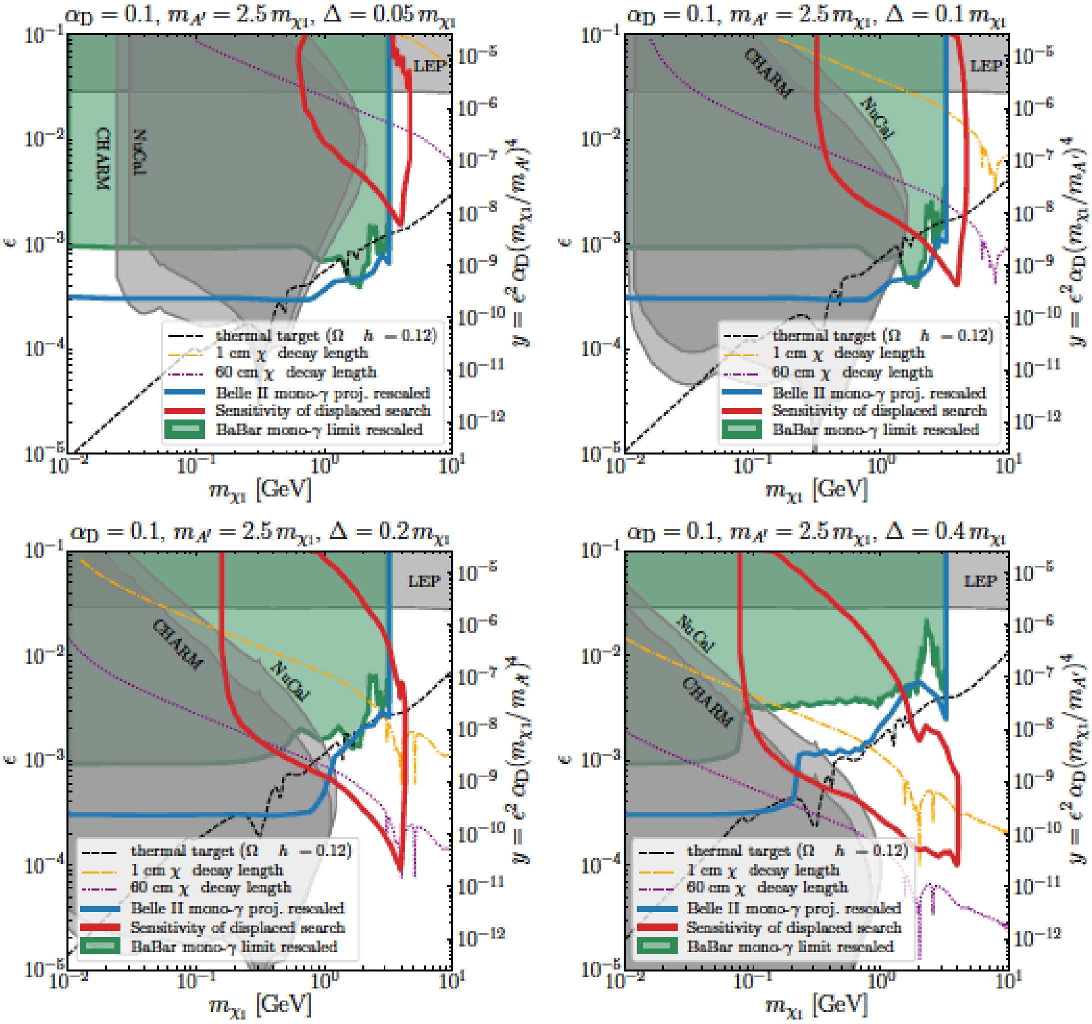


**Figure 6**: Sensitivity of Belle II to the parameter space of inelastic DM for an integrated luminosity of 20 $\text{fb}^{-1}$ for $m_{A'} = 2.5\, m_{\chi_1}$.

As expected, the search for displaced decays performs best precisely in the region of parameter space where the mono-photon signal is suppressed and promises substantial improvements in particular for large mass splitting $\Delta$. But even for small mass splitting there is substantial room for improvement at large DM masses, corresponding to photon energies that would be too small to be observed in the absence of an additional lepton pair. Indeed, the sensitivity of the search for displaced decays extends even into the off-shell region, where $m_{A'} > \sqrt{s}$. In this region the energy of the visible photon is no longer mono-energetic and peaks at $E(\gamma) \to 0$, making the conventional strategy to perform a bump hunt to search for dark photons impossible. In this region the presence of a displaced lepton pair is therefore essential.

Figure 7 shows the expected sensitivity for the 2 GeV cluster trigger, the three isolated clusters trigger, and the displaced vertex trigger separately for an integrated luminosity of

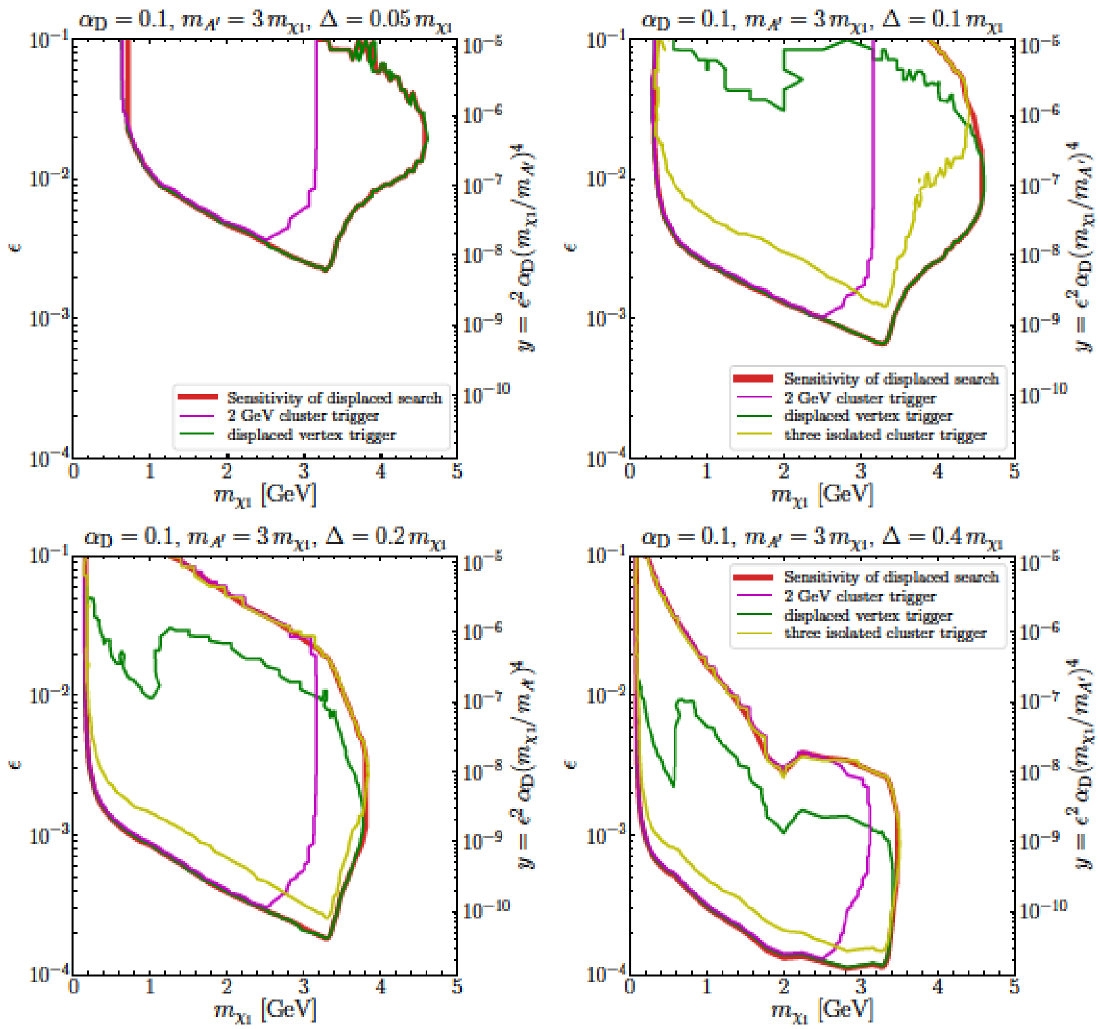


**Figure 7**: Sensitivity of the displaced search (same as figure 5, but with linear horizontal axis), overlaid with the regions where the various triggers are efficient for an integrated luminosity of 20 fb$^{-1}$ for $m_{A'} = 3.0\,m_{\chi_1}$.

20 fb$^{-1}$. For the smallest values of $\Delta$ the three isolated clusters trigger is inefficient, but it extends the sensitivity significantly towards higher masses for larger $\Delta$. The displaced vertex trigger has the best sensitivity for large values of $m_{\chi_1}$ and small $\epsilon$, whereas the three isolated clusters trigger adds additional sensitivity for large $\epsilon$. We note that the rather high $p_T$ and large opening angle requirement make the two-track trigger inefficient. Since the trigger rates of the three isolated clusters trigger are expected to be too high to sustain this trigger at the ultimate luminosities, we investigate the effects of a factor 10 prescale, i.e. randomly dropping nine out of ten events kept by this trigger. Figure 8 shows the expected sensitivity for the different triggers for an integrated luminosity of 50 ab$^{-1}$. The sensitivity loss due to this prescale at large values of $\epsilon$ is negligible.

Finally, we present our results in a different form in figure 9. Here the mass splitting $\Delta$

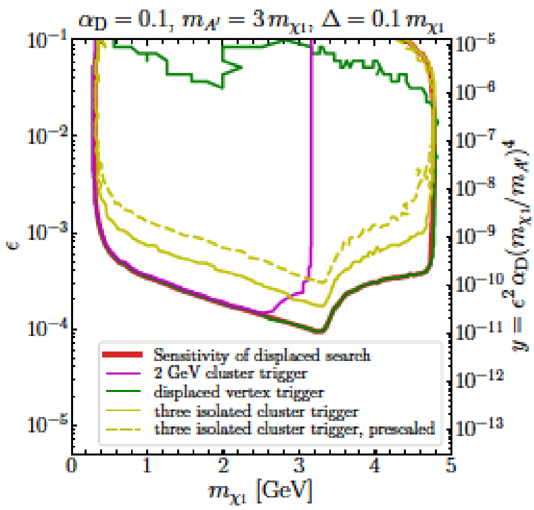


**Figure 8**: Sensitivity of the displaced search, overlaid with the regions where the various triggers are efficient for an integrated luminosity of 50 ab$^{-1}$ for $m_{A'} = 3.0\, m_{\chi_1}, \Delta = 0.1 m_{\chi_1}$.

is varied explicitly, while the value of $m_{\chi_1}$ is fixed to a different value in each panel. As in figure 6 the mass ratio is set to $m_{A'} = 2.5\, m_{\chi_1}$. Again, we observe a strong complementarity between the two different searches. The sensitivity of the mono-photon search decreases with increasing mass splitting, while the sensitivity of the displaced decay search improves. Intriguingly, the combination of the two searches will allow to probe the thermal target for a wide range of DM masses and mass splittings. We note, however, that this conclusion is specific to the assumed ratio of $m_{\chi_1}$ and $m_{A'}$. For $m_{A'} = 3\, m_{\chi_1}$, for example, the thermal target is already partially excluded by the constraint from BaBar (see figure 5).

## 4 Summary and discussion

The focus of the present work has been on the phenomenology of dark sectors that contain unstable but long-lived particles. An appealing example for such a dark sector are models of inelastic DM, in which a mass splitting $\Delta$ between two dark sector states $\chi_1$ and $\chi_2$ ensures that constraints from the CMB and direct detection experiments are evaded. The heavier state $\chi_2$ can have a decay length comparable to the typical size of particle physics experiments, making this model an interesting benchmark for searches for displaced vertices.

We have investigated the sensitivity of Belle II for the key signature of this model: a lepton pair originating from a displaced vertex in association with a single photon. We have identified the most sensitive detector regions and determined selection cuts that suppress the relevant backgrounds to a negligible level. We have furthermore calculated the sensitivity of mono-photon searches at Belle II and BaBar by determining the probability that $\chi_2$ escapes from the detector before decaying or that the decay products are too soft to be observed.

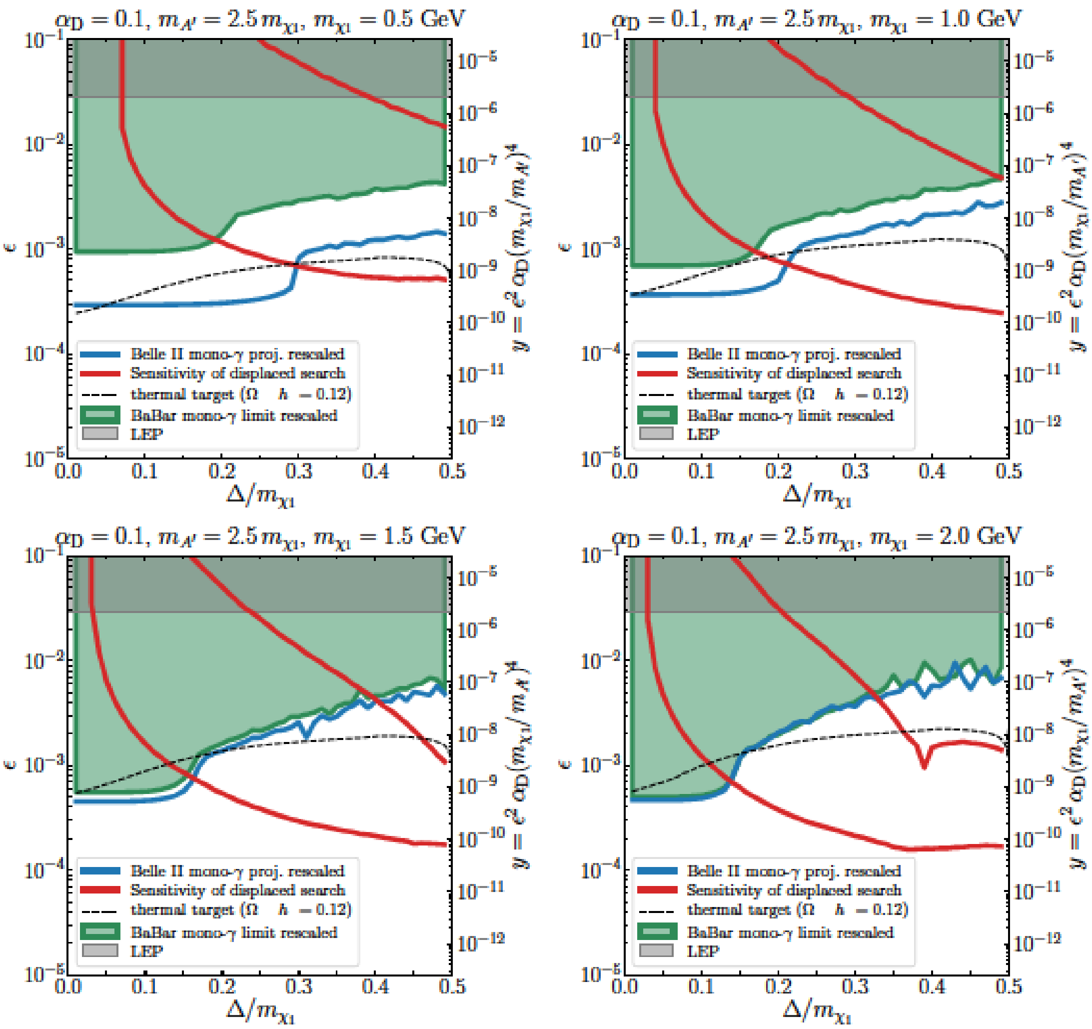


**Figure 9**: Sensitivity of Belle II to the parameter space of inelastic DM as a function of $\Delta$ for an integrated luminosity of 20 fb$^{-1}$ for $m_{A'} = 2.5\, m_{\chi 1}$.

Of course, Belle II is not the only experiment promising to probe deeper into the parameter space of inelastic DM. In figure 10 we show a comparison of the ultimate reach of Belle II (assuming an integrated luminosity of 50 ab$^{-1}$) with the projected sensitivities of various proposed experiments to search for long-lived particles. Note that most of the projections shown in figure 10 stem from experiments that are still in early stages of their development. Belle II in contrast is already taking data and should be able to provide first results within the next few years.

We emphasize that we assume $\Delta = 0.1\, m_{\chi_1}$ in figure 10 simply because this choice is commonly used in the literature for sensitivity estimates. The sensitivity of Belle II for different values of $\Delta/m_{\chi 1}$ are provided in figure 5 for an integrated luminosity of 20 fb$^{-1}$. For larger ratios $\Delta/m_{\chi 1}$, additional decay modes like $\chi_2 \to \chi_1 +$hadrons become important and the decay length of $\chi_2$ decreases rapidly. In this case the sensitivity of experiments

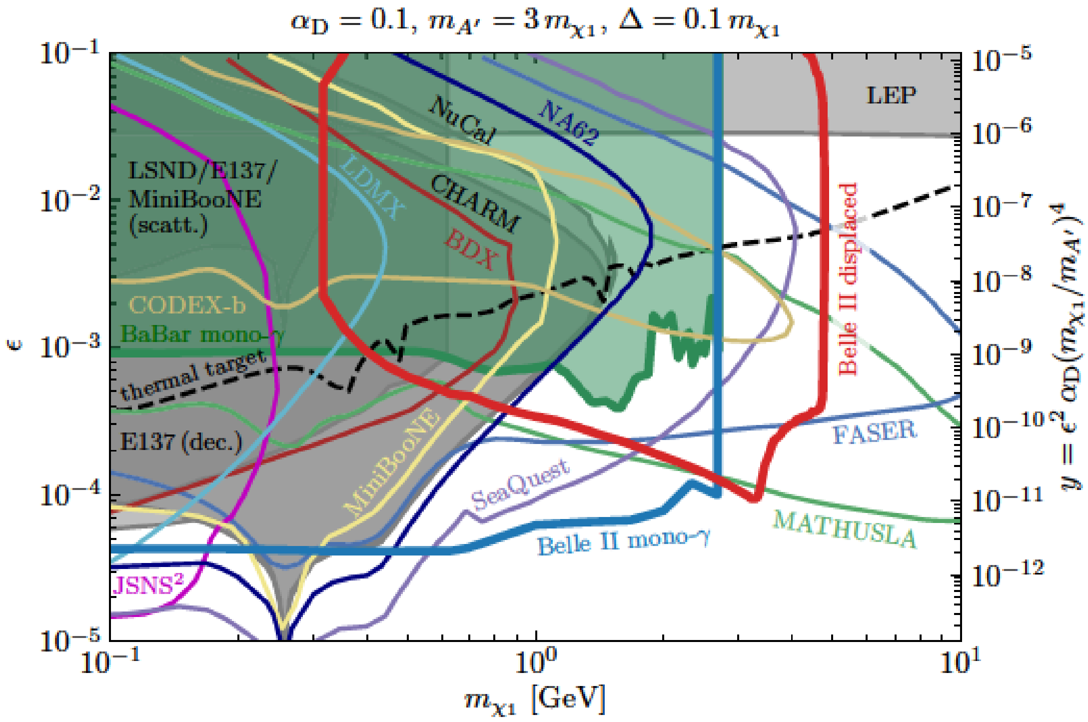


**Figure 10**: Comparison of our results with various other experiments. The Belle II results are given for $\mathcal{L} = 50\,\text{ab}^{-1}$: for the displaced search, the number of events is calculated with $\mathcal{L} = 50\,\text{ab}^{-1}$, i.e., assuming that this search is still background-free. For the mono-photon search, we rescale the previously found sensitivity with the $\sqrt[4]{\mathcal{L}}$.

like FASER (which requires a decay length of about 500 m in the laboratory frame) are strongly suppressed, while the displaced decay search at Belle II remains sensitive even for decay lengths below 1 cm. Moreover, the two different signatures discussed in the present work are highly complementary in the sense that the mono-photon search is most sensitive for small $\Delta$, while the displaced vertex search performs best for large $\Delta$ (see figure 9).

As part of this work we have also provided an improved calculation of the thermal target for inelastic DM, which is indicated by the black dashed line in figure 10. For the specific parameter combination chosen in this figure, large parts of the thermal target are already excluded by the mono-photon bound from BaBar. However, we have shown that this conclusion depends sensitively on the ratio of the DM mass and the dark photon mass (see figure 1) and that for example for $m_{A'} = 2.5 m_{\chi_1}$ the thermal target is essentially not probed by existing constraints (see figure 6).

Finally, we point out that the sensitivity of the displaced vertex search at Belle II relies crucially on the implementation of suitable triggers. We have identified a number of existing triggers that can in principle be used to search for displaced lepton pairs, but the trigger rate may be too high to make use of the full data set. There is hence clear need for the development of a dedicated displaced vertex trigger. By fully exploiting the potential

+ −

$+ \; -$

2003 + −
$tot$

+ −